J. Phys. E: Sci. Instrum., Vol. 12, 1979. Printed in Great Britain

An automated calorimeter for the temperature range 80–320 K without the use of a computer

FP spezifische Wärme

A Junod
Département de Physique de la Matière Condensée,
Université de Genève, CH-1211 Genève 4, Switzerland

Received 6 February 1979, in final form 17 May 1979

Abstract The continuous adiabatic method presented here yields, without the use of a computer, a graphical representation of the inverse specific heat as a function of temperature. The principal advantages are: simple construction, high-level electrical signals, small samples (about 1 g), good behaviour through first-order transitions, low additional masses, low cost and complete automation from about 80 to 320 K. The accuracy depends on the conductivity of the sample and varies between ± 1 and $\pm 3\%$. With more complex equipment, also described here, the conventional discontinuous heating method can also be used to obtain an extended temperature range (20–400 K) if required.

1 Introduction

Specific heat measurements in the temperature range from liquid nitrogen to boiling water provide useful information about such problems as the general shape of the phonon spectrum, the 'bare' electronic density of states at the Fermi level and the anharmonicity of the lattice. On a more qualitative level, for example, unstable superconductors such as the Chevrel phases often undergo phase transitions in this temperature range (Flükiger *et al* 1977). Thermal analysis probably is the most sensitive way of identifying these.

The difficulties that one must face when working in such an extended temperature range are connected, on the one hand, with heat exchange by radiation and, on the other, with the long times involved. The temperature span and the equilibrium times are larger than those usually encountered in liquid helium temperature work.

The solutions proposed for the first problem generally belong to two categories: either the heat losses are present, but balanced by a differential or ratiometric set-up (Yagfarov 1968, Marx 1978), or they are reduced to a negligible level by careful thermal shielding (e.g. Kleinclauss *et al* 1977). The second difficulty of long times is made acceptable by automation, using either data acquisition or some sort of analogue processing. For example, if the sample is forced to follow a linearised temperature ramp, the input power directly represents the specific heat (Bochirol *et al* 1971).

Depending on the specific problem at hand, the published designs have various advantages or drawbacks. The linear temperature ramp method does not behave well when passing a first-order phase transition. Data acquisition is probably best but clearly expensive; in any case much time must be spent in the development of real-time programs. Differential techniques, of course, have a high degree of differential resolution, but the precision in the absolute mode generally suffers because of the additional masses. A common source of error is the asymmetry of the relaxation times. Most designs must use very complex electronics to handle thermocouple signals at the nanovolt level (Hall *et al* 1975).

We tried to avoid these drawbacks when designing our apparatus. The present method has several main advantages:
the measurement is based on a straightforward first-principle method;
the corrections for additional masses are low, equivalent to about 85 mg of copper;
the level of the electrical signals is high;
the data appear graphically on an X–Y recorder;
the cost is low – no computer is required;
the geometry used speeds up the attainment of internal equilibrium within the sample: a run for a reasonably good heat conductor lasts only 4–5 h;
the behaviour through a first-order phase transition is excellent.

It has the following main limitations:
the temperature range in the sweep mode runs only from about 80 to 320 K;
the scales of the graph are slightly distorted;
the preparation of the sample for a run takes some time since there is no sample holder.

2 Calorimeter

Figure 1 shows the arrangement used. The sample is suspended by three silk threads inside a copper shield Sh: its weight normally ranges from 0·5 to 5 g. A miniature platinum thermometer T_1 (model 118MF/500 Ω†) is glued on to it with varnish and covered with a thin copper foil to improve the thermal contact with the sample. The sample heater H_1 is a thin carbon film painted on to a layer of varnish. Its high resistance (about 2 kΩ at room temperature) makes a two-lead configuration to the heater acceptable; furthermore the heater area can be made a substantial fraction of the sample area, ensuring good thermal contact and fast equilibration. Typical extra masses, besides the thermometer, consist of 2–3 mg of varnish, 15–20 mg of copper, about 0·1 mg of carbon and an ill defined part corresponding to the electrical leads. They can be measured in a separate run without any load. The six electrical leads are 50 μm constantan wires; their resistance is approximately 10 Ω per lead to the heater and 30 Ω per lead to the thermometer. They are anchored to 1·2 mm diameter insulated copper wires tightly fitted into holes which are drilled in the upper platform of the shield; varnish is used to improve the thermal contact.

The cylindrical adiabatic shield is fastened to the top of the vacuum can by a thin-walled stainless steel tube. Its small size (30 mm diameter, 1 mm thickness) ensures a fast response. The upper plate bears the thermal anchorings, a second platinum thermometer T_2 and a heater H_2. A heater H_3 is wound around a part of the can which may be unscrewed to give access to the experimental space. The thermal contact through the thread is crucial: the surface oxide is removed with a glass-fibre brush and the contact area is coated with thermally conducting grease. Small holes facilitate the evacuation of the shield.

† Manufactured by Rosemount Inc., PO Box 35129, Minneapolis, Minnesota 55435, USA.

0022-3735/79/100945+08 $01.00

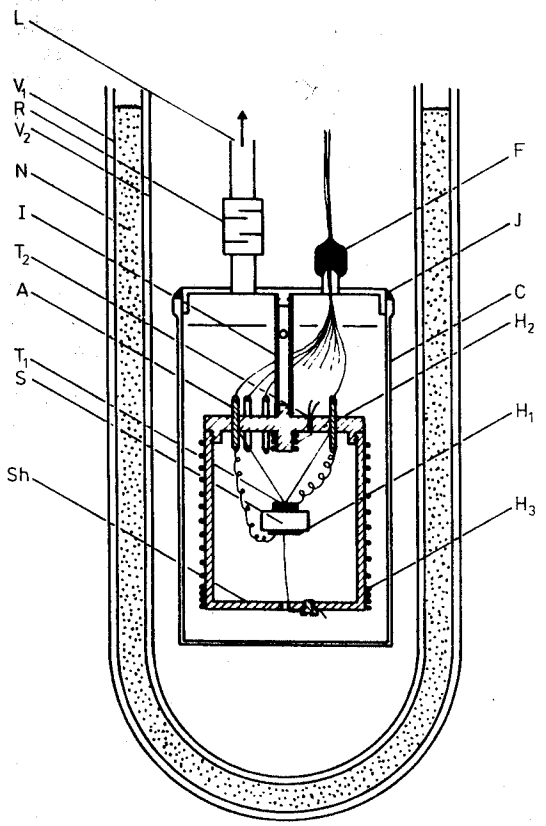

Figure 1 Scheme of the calorimeter. V_1: outer Dewar vacuum space; V_2: inner Dewar vacuum space; N: liquid nitrogen; R: radiation trap; L: pumping line; F: electrical feedthrough; A: thermal anchorings; C: vacuum can; J: soft-solder joint; S: sample; T_1: sample thermometer; H_1: sample heater; T_2: shield thermometer; H_2, H_3: shield heaters; I: stainless steel holder; Sh: copper adiabatic shield.

The outer can is sealed with $In_{52}Sn_{48}$ solder. Other demountable seals could of course be used here. The electrical feedthrough consists of a plug resin (Stycast 2850GT†) attached to a thin-walled copper tube. It is vacuum-tight down to 4 K. The space between the can and the Dewar contains liquid helium during a low-temperature run (20–100 K) or simply nitrogen gas during a 'high'-temperature run (above 80 K). The outer vessel is filled with liquid nitrogen.

3 Measuring method

The can is evacuated with an oil diffusion pump provided with a nitrogen-cooled vapour trap. The outer Dewar is filled with liquid nitrogen and the sample cools to 80 K by radiation overnight. If operation down to 20 K is required, 1 litre of liquid helium is transferred into the inner Dewar; some exchange gas will then cool the sample to 5 K in a few minutes. The can is then continuously pumped during the measurement to about 10^{-5} Pa (10^{-7} Torr). The electrical connections are sketched in figure 2. Two independent regulated current sources supply roughly 0·3 mA to the platinum thermometers in a four-lead configuration. The power dissipated in the sensors is about 40 μW at room temperature and 8 μW at 80 K; it remains at least two orders of magnitude below the heater power. This relatively large measuring current results in very convenient high-level signals (100 mV at 200 K) while self-heating effects remain negligible. The apparent change in temperature when the power dissipated in the sensor attached to a sample varies from 0·2 to 45 μW is less than 0·01 % at room temperature.

The current in the shield thermometer T_2 is adjusted once in order that under equilibrium conditions at room temperature the voltages across both thermometers match exactly. Since the normalised resistance curve of the sensors is very close to ideal, the voltages will then match at any temperature to within a small fraction of a degree – especially at higher temperatures where it is most important. An efficient temperature controller ensures that both voltages are equal to within 1 μV ($1:10^5$) under steady state conditions. This cancels heat conduction along the leads (the sensor is close to the thermal anchorings) and also the heat losses by radiation if the heating power is well distributed along the walls of the shield. We shall return to this later.

The conditions are thus very close to adiabatic, and the degree of adiabaticity can be easily checked. Two methods can now be used.

† Supplied by Emerson and Cuming, Nijverheidsstraat 24, Oevel, Belgium.

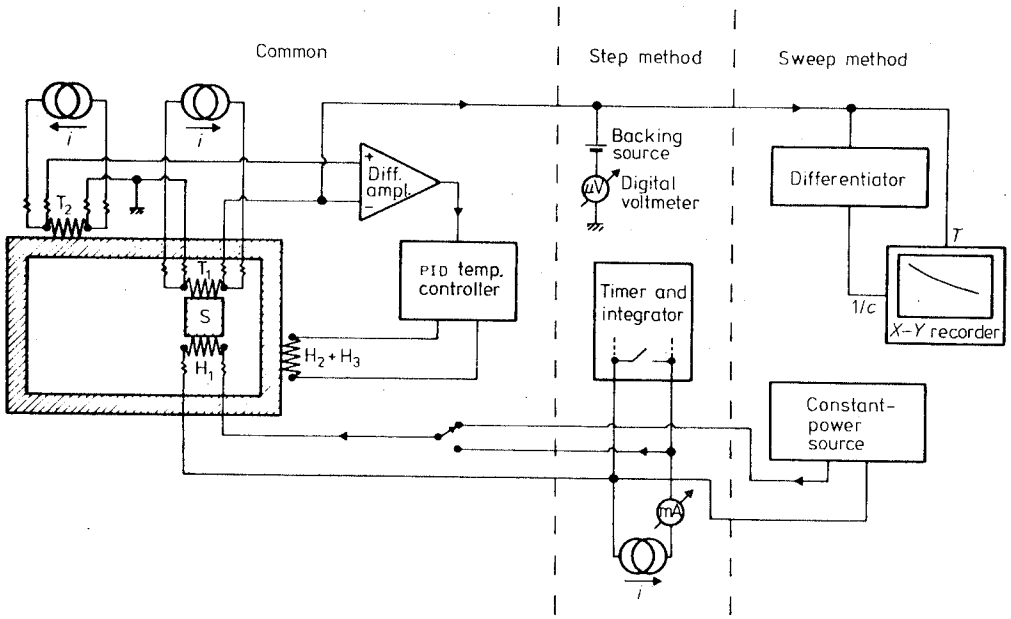

Figure 2 Electrical circuit.

3.1 *Sweep method*

A constant power P is supplied to the sample. Let $\dot{Q}$ be the heat exchanged with the surroundings by conduction and radiation. The regulation loop of the thermal shield ensures that $\dot{Q} \ll P$ (for the typical data shown in figure 4, $\dot{Q} \approx 50\ \mu W$ and $|\dot{Q}/P| < 1\%$). Then

$$P + \dot{Q} = mc\dot{T}, \tag{1}$$

where m and c are the mass and specific heat of the sample. An analogue differentiator then reads a voltage drift $\dot{U}$ across the thermometer. If the heater power is turned off, then

$$\dot{Q} = mc\dot{T}_0 \tag{2}$$

and the voltage drift will be $\dot{U}_0 (\ll \dot{U})$. Hence

$$\frac{1}{c(T)} = \left(\frac{m}{PI}\frac{dT}{dR}\right)(\dot{U}(T) - \dot{U}_0(T)) \tag{3}$$

where I is the thermometer current and dR/dT the temperature coefficient of the platinum resistor.

As a first approximation, this coefficient can be considered as constant ($0{\cdot}041\ R_{273} \pm 5\%$) from 75 to 350 K, and $\dot{U}_0$ can be neglected. $\dot{U}$ is then proportional to c^{-1} and a plot of $\dot{U}$ against U provides a representation of c^{-1} against T. The slight nonlinearities on both scales are due to the nonlinearity of the thermometer itself. The run lasts 3–9 h without any manual intervention. Deviations from a smooth curve by as little as 2% can be resolved and transition temperatures can be localised to within 1 K on the plot.

The graph can be very rapidly corrected for precise determinations. Equation (3) must then be used without approximations. P is corrected for the losses in the current leads (about 0·5%). $\dot{U}_0(T)$ is recorded at 100 and 300 K by turning off the heater power for a few minutes. The resulting points on the plot define a baseline which must be subtracted from the $\dot{U}(T)$ curve. dR/dT is given in table 1 for the evaluation of c at selected temperatures.

Beyond 320 K, adiabatic conditions degrade rapidly and the baseline should be checked more frequently. This is the most important temperature limitation since the thermometer itself will withstand 670 K. The calorimeter we have used so far has not been optimised; for example, the inner surface of the copper shield has not been gold-plated. Anchoring the leads from the outer can on an independently regulated thermal block, using a *long* cylindrical shield and gold-plating all the surfaces should make it possible to push the temperature limit to significantly higher values.

However, trimming was found necessary to minimise heat leaks. The feedback loop can only ensure that the two regions close to T_1 and T_2 are at the same temperature but, depending on the distribution of the heater windings and of the masses, the walls of the shield may lead or lag behind the sensor. As the shield heater is split in two parts, we can adjust the distribution of power by a resistor network. This was done in worst-case conditions, e.g. with the shield very loosely screwed and no thermal grease on the thread. Thermometer T_1 was pressed against the cylindrical wall of the shield, a constant voltage comparable to that found in a typical run was applied to both heaters in series and some current was diverted from one of the heaters until the temperature difference between T_1 and T_2 was smallest in the largest possible temperature domain (more weight was put in the higher temperature range).

A plot of the inverse specific heat does not allow a precise determination of the latent heat L at a phase transition. This drawback can be overcome if the time elapsed during the transition, Δt, has been recorded. Let us suppose that the transformation starts at a temperature T (thermometer voltage: U) and ends at a temperature $T + \Delta T$ (thermometer voltage: $U + \Delta U$). Let c_m be the mean 'baseline' specific heat outside the peak and $\dot{T}_m$ the corresponding heating rate. Then

$$\begin{aligned} L &= \int_T^{T+\Delta T} (c(T) - c_m)\, dT \\ &= \frac{P}{m}\int_T^{T+\Delta T} \left(\frac{dT}{\dot{T}} - \frac{1}{\dot{T}_m}\Delta T\right) \\ &\approx \frac{P}{m}\left(\Delta t - \frac{\Delta U}{\dot{U}_m}\right). \end{aligned} \tag{4}$$

The implicit hypotheses are that (1) c_m can be uniquely defined, (2) the adiabatic conditions are fulfilled, e.g. $\dot{Q} \ll P$, and (3) the sensitivity of the thermometer dR/dT does not vary appreciably over ΔT, which is generally true (see table 1). ΔU and $\dot{U}_m$ are read on the plot; a time recording of $\dot{U}$ gives a good determination of Δt.

Other designs for continuous calorimetry (Bochirol *et al* 1971) and regular differential thermal analysis (DTA) use constant-$\dot{T}$ rather than constant-P sweeps. Stability problems in the regulation loop may then arise when crossing first-order phase transitions since the heating power should in principle reach an infinite value during a negligibly short time. One advantage of our method is that these transitions are passed at a vanishing speed, thereby helping to maintain thermal equilibrium.

An extension of the sweep method to powdered samples has proven possible. A thin-walled capsule which can contain 1·7 cm³ of sample was machined from solid commercial silver. Besides its high conductivity and high reflectivity, silver has a relatively low heat capacity per unit volume. The filled cell is sealed with a Teflon gasket under a suitable pressure of exchange gas and then treated as a bulk sample. Heating rates as low as 5 mK s^{-1} can be used without difficulty. Because of the large mass of the full cell (about 10 g) and the high reflec-

Table 1 Temperature coefficient of the normalised resistance of pure, annealed, strain-free platinum, and heat capacity of the additional masses. The thermometer leads are shortened until the total mass is 84·0 mg.

T (K)	$(1000/R_{273})(dR/dT)$ (K^{-1})	C_a (mJ K^{-1})
20	0·743	1·02
30	1·905	2·35
40	2·988	3·86
50	3·704	5·36
75	4·307	9·1
100	4·315	12·4
125	4·242	15·8
150	4·180	18·6
175	4·127	21·4
200	4·083	23·6
225	4·045	25·5
250	4·012	26·8
275	3·981	27·6
300	3·952	28·5
325	3·923	29·7
350	3·893	30·6
375	3·864	(31·4)
400	3·835	(32·5)

tivity of the surface, the baseline drift still remains below 1% of the useful signal. The cell ensures that the surface of the sample is isothermal, a very favourable condition as will be seen in §4. The heat capacity of the empty cell must be determined in a separate run.

3.2 *Step method*

The classical discrete heating method can also be used here; it has been described in numerous articles (e.g. Kleinclauss *et al* 1977). A known amount of heat ΔQ is supplied electrically for 1–4 min. The temperature drifts are recorded before and after the heating period; the shield regulation maintains them at the millikelvin level. The net temperature increase ΔT is found by extrapolation into the middle of the heating period. The heat capacity is then $mc = \Delta Q/\Delta T$.

In a limited temperature range, the temperature drift can be cancelled by offsetting the input of the temperature controller. Using a digital voltmeter with 100 nV resolution for temperature read-out, temperature steps as low as 20 mK can be resolved to 1%. This high resolution can be valuable in the study of critical parameters near a second-order transition.

We have used this method extensively during the development phase of the apparatus. The points in figure 3 are an example. We now find no advantage in using it where the sweep method works. The regulation loop of the radiation shield no longer works in stationary conditions and time-dependent temperature gradients in the shield and in the sample may cause uncontrollable systematic errors.

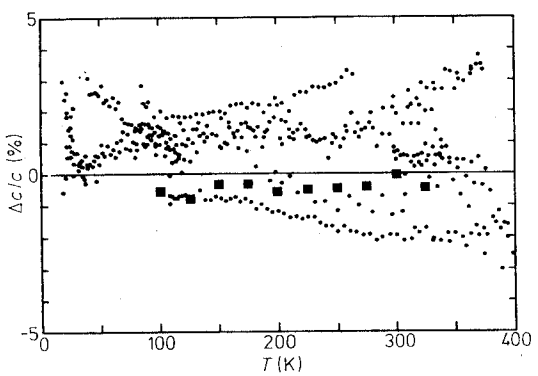

Figure 3 Specific heat of copper: deviation plot with respect to Furukawa's selected values (Furukawa *et al* 1971, Pawels and Stansbury 1965). The squares refer to the sweep method.

4 Results

4.1 *Specific heat of the extra masses*

Thermometer T_1 was wrapped in an 11 mg copper foil using 2·5 mg of a varnish similar to GE 7031. A heater was painted on to the foil. The total mass was only 85·4 mg, but the sweep method could still be used satisfactorily above 80 K. The power supplied to the sample was 0·469 mW ± 0·5%. Due to the small heat capacity, the baseline drift had to be checked more frequently; it varied smoothly from 2% at 100 K to 10% at room temperature and 25% at 360 K. Below room temperature, it can be verified that the drift is mainly caused by the thermometer current. From 20 to 100 K, the specific heat of the extra masses was determined by the step method. The overlap is excellent. The scatter of the data is 2% RMS below 100 K and 1% above 100 K. Selected values are shown in table 1. Generally speaking, measurements on 0·1 g samples seem quite feasible.

4.2 *Specific heat of copper*

Over one year's use, about 500 data points were taken on 99·999% pure copper. Four different samples from 0·58 to 4·4 g were prepared; two different platinum thermometers were used alternatively; the manipulations were carried out by two independent experimenters and two different designs of temperature controller were tested. Helium exchange gas was used in some cases. The scatter of all these data about accepted values (Furukawa *et al* 1968, Pawels and Stansbury 1965) is shown in figure 3 and it seems reasonable to evaluate the accuracy of the step method as ±2·5% from 25 to 400 K.

The reproducibility in the sweep mode, which was used in a more recent measurement, seems better; the data taken on a 1·5 g copper sample are consistently 0·4% below Furukawa's selected values with very little scatter. They appear in figure 3 as squares.

Copper does not provide a very stringent test due to its high conductivity. A discussion of the possible systematic errors in more general cases will be given in §5.

4.3 *Typical results*

Figure 4 illustrates an advantage of the sweep method. A 1·2 g sample of LuCuAl was studied. Figure 4(*a*) was obtained by the discontinuous heating method. What appears as an unlucky point to be rejected near $T = 232$ K was confirmed to be a real peak in the specific heat by the continuous run shown in figure 4(*b*). The data points obtained at selected temperatures from the latter measurements appear as squares in figure 4(*a*). They agree to within 0·5% RMS.

Figure 5 shows a first-order phase transition in $Cu_2Mo_6Se_8$. The specific heat increases by a factor of 10 within a small temperature interval. In a run using the step method, unexpected long relaxation times near the peak would make any

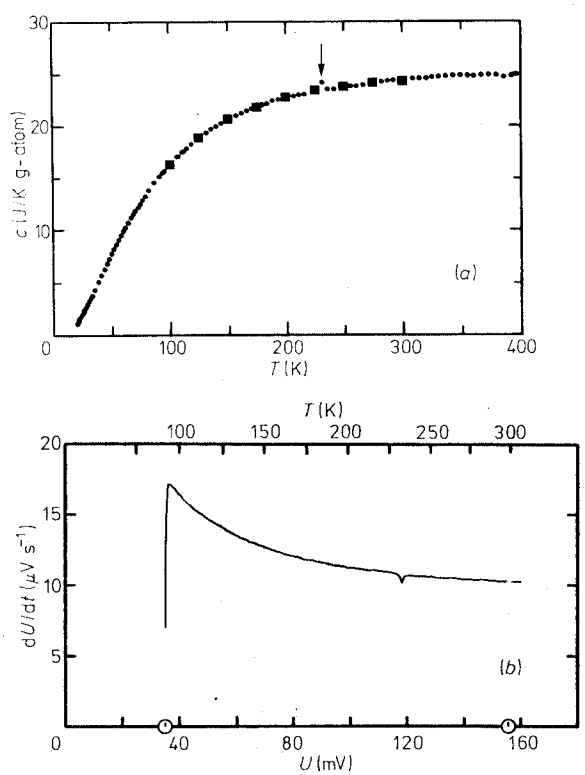

Figure 4 Specific heat of LuCuAl: (*a*) results of the step method; (*b*) raw results from the sweep method. The latter data are shown in (*a*) as squares after evaluation at selected temperatures.

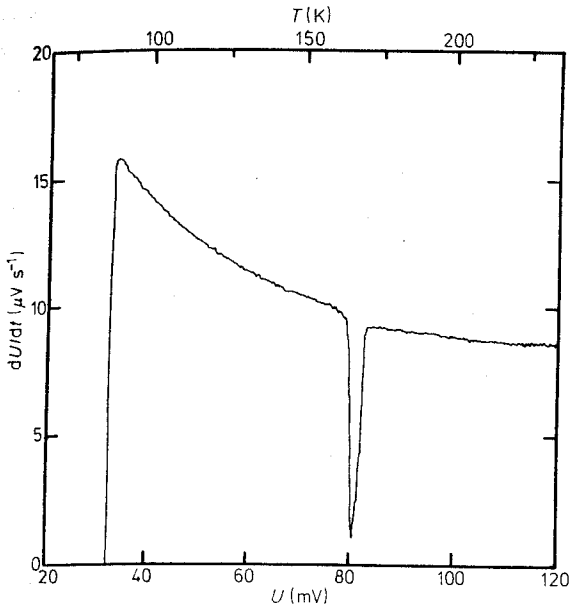

Figure 5 Specific heat of $Cu_2Mo_6S_8$ showing a first-order phase transition near 168 K.

systematic data acquisition rather complicated. Here the temperature remains almost constant for a long time and fine structures due to the transitions of the individual crystallites can be discerned. The first-order nature of this transition is supported by the hysteresis of the resistivity (Flükiger 1976 private communication).

5 Discussion of systematic errors

We shall discuss two categories of errors. The first one plays a role in all measurements, the second one appears only when measuring badly conducting samples. We implicitly refer to the sweep method only and evaluate the errors at room temperature.

A first error of electronic origin is due to the heavy filtering that must precede the differentiation of the thermometer voltage. It is easy to show that under steady state conditions where the temperature increases linearly, the output of the first-order filter will lag behind the input signal by exactly one time constant. If the temperature stops increasing, as it will do in the case of a latent heat, this lag will vanish. With typical values, e.g. 10 s time constant and 20 mK s^{-1} heating rate, this will cause a 0·2 K temperature error. As the 'temperature' channel of the recorder is in fact connected to the output of the filter, this source of error will usually be negligible.

The temperature error due to the thermometer itself, including that caused by the current supplies, digital voltmeters and input bias current of the amplifiers, can be checked from time to time by dipping the platinum sensor T_1 into an oil bath at room temperature. After about 50 thermal cycles and over one year's use, the drift was near 0·5 K. The effect of this slope error on the specific heat will be 0·17%.

The total error of the differentiator and the X–Y recorder was also checked eight months after initial calibration using a slow triangular-wave generator, a digital voltmeter and a time counter; it was about +0·3%.

It was noted that the degree of adiabaticity could be checked when the power supplied to the sample was reduced to zero. However, under dynamic conditions this point has to be considered more carefully. Let us suppose that at zero power the thermometers T_1 and T_2 are ideally matched and that the temperatures in the sample and in the shield are homogeneous. The net heat exchange with the surroundings is then zero. We now consider the stationary case some time after the sample heater has been turned on when the temperature is linearly increasing. Three gradients will appear: the first one across the layer of varnish that insulates the heater from the sample, the second one across the sample and the third one in the layer of varnish that separates the sample from the thermometer. Some surfaces will then lose heat by radiation because their temperature is higher than that of the thermometer (which is identical to that of the shield). The heat conduction along the constantan wires is at least three orders of magnitude below the radiation losses and at room temperature can be completely neglected.

The varnish/thermometer system is roughly equivalent to an RC circuit (figure 6). From the mass, area and thermal

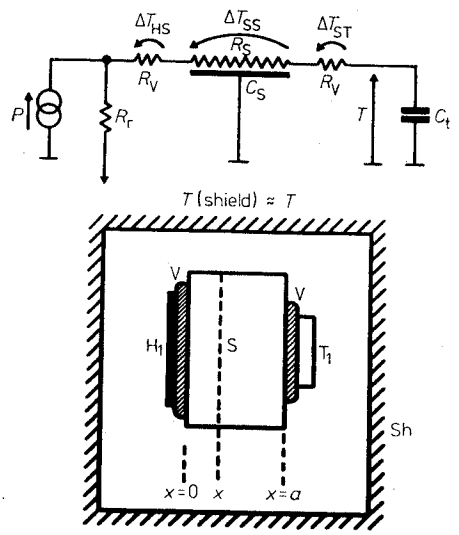

Figure 6 Diagram of the sample assembly and equivalent electrical circuit. V is a layer of varnish about 0·1 mm thick; R_V is its thermal resistance; R_S and C_S are the sample thermal resistance and heat capacity respectively. C_t is the thermometer heat capacity and R_r the radiation resistance as given by $R_r=(4\alpha S\sigma T^3)^{-1}$.

conductivity of the varnish and from the known heat capacity of the thermometer, we estimate that this time constant is close to 1 s. The internal time constant of the thermometer, which is given by the manufacturer as 0·3 s between 300 and 350 K, can be neglected here. In a typical experiment, the temperature of the sample – if it is a good heat conductor – will then be $\Delta T_{ST}=20$ mK above the shield temperature. The power lost by radiation will then be

$$P=4\alpha S\sigma T^3\Delta T. \qquad (5)$$

Assuming a (bad) absorption factor $\alpha\approx 0{\cdot}6$ and a sample surface area $S=1$ cm² (σ is the Stefan–Boltzmann constant), it amounts to approximately 7 μW. This is about equivalent to a 0·1% error in the heater power.

Because of the large contact area, the temperature difference between the heater and the sample is not really a problem. Typically 10 mW of heat power are injected through a 30 K W^{-1} thermal resistance. The surface of the heater is then $\Delta T_{HS}=0{\cdot}3$ K above the sample temperature. With $S=0{\cdot}2$ cm², equation (5) indicates that the heater radiates about 0·25% of its power. This error could in principle be eliminated if the black surface of the heater were covered with a thin copper foil attached to the sample.

Let us recall that the steady power input through the thermometer measuring current is fully accounted for if the drift with the heater switched off has been recorded.

The most serious problem is sample-dependent: it involves the thermal conductivity of the material to be investigated. Assuming a one-dimensional geometry, which is not unreasonable in view of the large area of the heater (figure 6), it can be shown that

$$T(x,t)=\frac{P}{mc}\left[\frac{x}{\lambda}\left(\frac{x}{2}-a\right)+t\right] \tag{6}$$

where P is the input power in the plane $x=0$, c is the heat capacity (J K^{-1}), λ is the coefficient of diffusivity (m^2 s^{-1}) and T is the temperature in the x plane at time t. The hypotheses used here are: that P, λ and c are constants: that there are no lateral losses and the thermometer end of the sample ($x=a$) is also thermally insulated; and that the investigation is in the asymptotic regime where $\dot{T}$ is constant.

The temperature difference between the extremities of the sample is then

$$\Delta T_{SS}=Pa/2wS \tag{7}$$

where S is the cross-section of the cylinder and w its thermal conductivity (W K^{-1} m^{-1}). Most radiation losses will occur in the $x=0$ plane and the error can be estimated:

$$\frac{P(\text{radiated})}{P(\text{supplied})}=\frac{2\alpha\sigma T^3 a}{w}. \tag{8}$$

It is directly proportional to the length of the sample. The best geometry is that of a disc. With a thickness $a=4$ mm, the error will be about 2×10^{-5} for copper, 5×10^{-4} for stainless steel and 3×10^{-2} for a PTFE sample at room temperature. This last example was chosen deliberately since the macroscopic thermal conductivity of a molten sample of the Chevrel-phase $Cu_2Mo_6Se_8$ is about the same as that of Teflon (unpublished work). These errors are independent of the heating rate, and the only way to avoid them is to use some high-conductivity coating, or the silver capsule described in §3. As a conclusion, when measuring about 0·01 g-atom of a well behaved metal, the systematic errors of the sweep method can be estimated to within 1% at room temperature, including the uncertainty in the additional masses. In special cases, the thermal conductivity should be estimated, for example from the response to step heating.

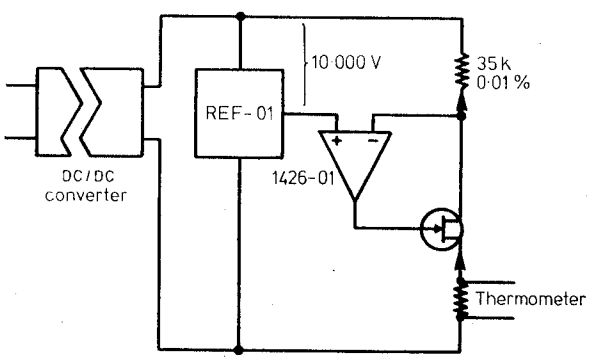

Figure 7 Block diagram of the current source. The integrated circuit REF-01 is a precision voltage reference.† The module 1426–01 is an FET input operational amplifier.‡

† Manufactured by PMI, 1500 Space Park Drive, Santa Clara, California, 95050, USA.

‡ Manufactured by Teledyne Philbrick, Allied Drive, Route 128, Dedham, Massachusetts 02026, USA.

6 Electronics

A number of electronic devices based on operational amplifiers were built in our laboratory. In some cases the specifications needed were not met by commercially available apparatus or only in too elaborate and expensive equipment.

6.1 *Current sources*

The current through the thermometers must stay constant to within 0·01% per day and within 10 ppm over shorter periods (a temperature step). The block diagram of a simple current source is shown in figure 7. The integrated circuit REF-01 gives a 10 V reference voltage stable to within 3 ppm K^{-1}. An FET-input operational amplifier compares the reference voltage with that developed by the load current across a 35 kΩ metal resistor. The amplified error signal drives a field-effect transistor in series with the load. A DC/DC converter supplies the power, ensuring truly floating operation.

6.2 *Constant-power source*

The design sketched in figure 8 stabilises the output power to within ±0·5% when the load resistance varies from 700 to 4000 Ω in the power range generally used (10–20 mW). In a typical sweep from 80 to 350 K, the power delivered to the

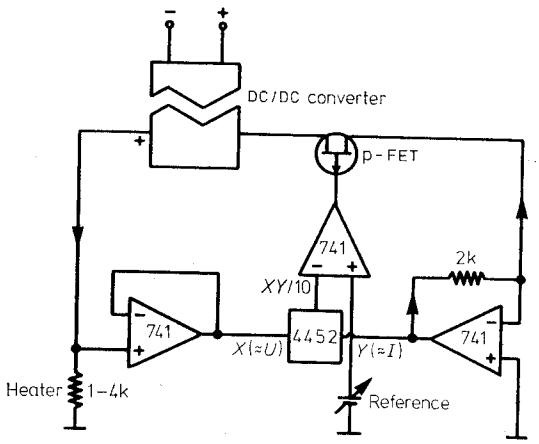

Figure 8 Block diagram of the constant-power source. The module 4452 is a general-purpose multiplier (Teledyne Philbrick).

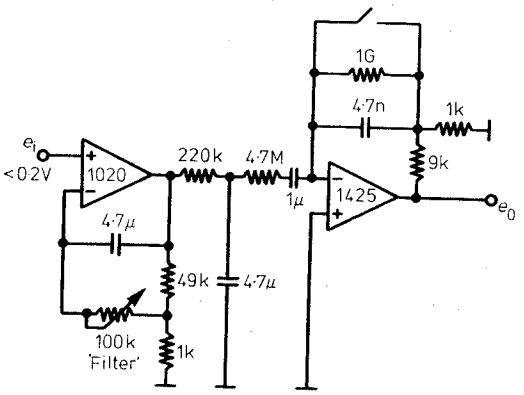

Figure 9 Block diagram of the differentiator. The modules 1020 and 1425 are operational amplifiers (Teledyne Philbrick). $e_0=5\times10^5\,de_i/dt$.

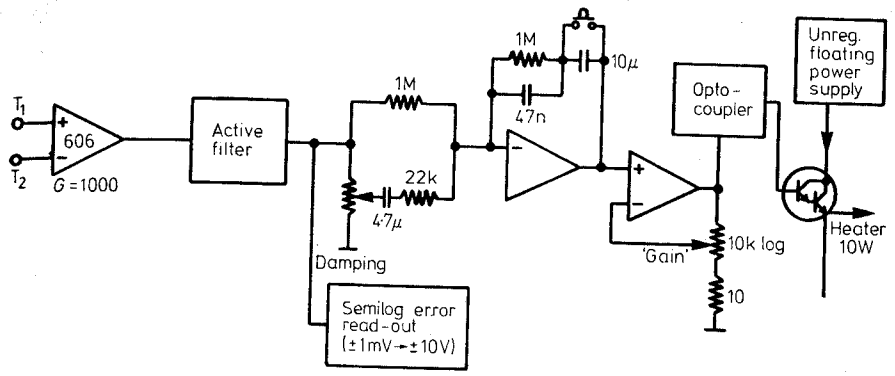

Figure 10 Block diagram of the temperature controller. The module 606M is an instrumentation amplifier.†

heater stays constant to within 0·1%. The circuit constantly computes the product UI with an analogue multiplier and compares it with a reference. The amplified error signal controls an FET in series with the load.

6.3 *Differentiator*

A typical heating rate at room temperature is 20 mK s^{-1}, yielding a voltage derivative $\dot{U} \approx 10^{-5}$ V s^{-1}. One per cent of this value corresponds to 3 V per year. This is about equivalent to the noise referred to the input of the following differentiator (figure 9) with minimum filtering. The input signal is brought to the 10 V level by a low-drift low-noise operational amplifier; it is filtered with a time constant that can be adjusted up to 25 s. The differentiating stage uses a low-bias-current low-noise FET amplifier. The capacitor C (1 μF) is a critical element; its insulation resistance must exceed 10^{11} Ω. The equivalent derivative time constant is 5×10^5 s.

With maximum filtering, the output will reach 99% of its asymptotic value 2 min after a step function in $\dot{U}$ is applied to the input. This restriction should only be important in the recording of sharp phase transitions.

6.4 *Temperature controller*

Reproducible results depend on the response of the adiabatic shield to a temperature step. The controller described here proved to be reliable, and regulation to within 10 ppm was possible without adjustments or instabilities up to 400 K.

To avoid any possibility of electrical feedback through common ground leads (the gain can be as high as 10^8 at 3 Hz), the controller was built in three sections – preamplifier, controller, power stage – each having its own power supply. An optocoupler between the last stages floats the output. The overall gain normally used is between 2×10^5 and 5×10^5 in the proportional band. The preamplifier is an instrumentation amplifier chosen for its low noise (about 1 μV peak-to-peak) and low drift (0·25 μV K^{-1}); it is operated with a gain of 1000. This is the only critical part. The block diagram of the controller is shown in figure 10; cheap bipolar and FET operational amplifiers are used throughout.

The response to a 1 mK temperature error ranges from 20 to 100 mW in the proportional band, depending on the mean temperature and power level. The steady state temperature error, which would lie between 30 and 120 mK with the gain normally used, is reduced to a negligible level by the integrating action of the controller. The derivative action corrects the phase response of the loop and adds gain at frequencies of the order of 1 Hz. This speeds up the regulation and damps any incipient oscillatory behaviour.

† Manufactured by Analog Devices, Route 1, Industrial Park, PO Box 280, Nordwood, Massachusetts 02062, USA.

7 Conclusion

Derivative analysis is not new (Cochran *et al* 1966, Pompe and Hegenbarth 1968, Hall *et al* 1975, Moses *et al* 1976). When compared with other designs, this calorimeter has three essentially new features.

(i) The use of essentially linear thermometers which give a signal level one order of magnitude higher than thermocouples, and which are less susceptible to degradation by repeated manipulations. The effect of spurious thermal voltages, noise, AC pick-up and amplifier drifts is thus minimised. This makes analogue derivation possible.

(ii) The extensive use of modern, cheap, operational amplifiers.

(iii) The use of large-area, negligible-mass heaters that speed up thermal equilibration within the sample without adding parasitic heat capacity.

Presently the main limitation is the temperature range, but the upper limit could be pushed 100 K higher by a more thoughtful design.

The realisation presented here is mechanically simple, allows precise step-by-step measurements from 20 to 400 K and automatic survey of the range 80–320 K. It should be useful especially in the search for low-temperature phase transitions, for the determination of Debye temperatures near $\theta/2$, for the study of anharmonicity and high-temperature electronic contribution to the specific heat, etc. It might be considered by metallurgists as a quantitative alternative to low-temperature DTA, a precious tool in establishing low-temperature phase diagrams.

Acknowledgment

I am very thankful to Mr Ch Burgisser who assembled and wired all the electronic devices, to Mr B Lachal for his cooperation and to Professor J Muller for his interest in this project. This work was supported by the Swiss National Science Foundation.

References

Bochirol L, Bonjour E, Lagnier R and Pierre J 1971 Technique de mesure de chaleur spécifique en méthode dynamique continue (4–300 K)
Congr. Int. du Froid, Washington, Centre d'Etudes Nucléaires de Grenoble Note SPCBT 228/71

Cochran J F, Shiffman C A and Neighbor J E 1966 Specific heat measurements in 1–10 K range using continuous warming method
Rev. Sci. Instrum. **37** 499

Flükiger R, Junod A, Baillif R, Spitzli P, Treyvaud A, Paoli A, Devantay H and Muller J 1977 The low-temperature phase diagram of the system $Cu_xMo_6S_8$ in the range $1{\cdot}5 \leqslant x \leqslant 3{\cdot}55$
Solid St. Commun. **23** 699

Furukawa G T, Saba W G and Reilly M L 1968 Critical analysis of the heat capacity data of the literature and evaluation of thermodynamic properties of copper, silver and gold from 0 to 300 K
Nat. Bur. Stand. Ref. Data Ser. **18** 1

Hall R A O, Lee J A, Mortimer M J and Sutcliffe P W 1975 The measurement of specific heats at low temperatures by an adiabatic technique
Cryogenics **15** 129

Kleinclauss J, Mainard R and Fousse H 1977 Sensitive adiabatic calorimeter for measurement of low-temperature specific heats
J. Phys. E: Sci. Instrum. **10** 485

Marx R 1978 A simple and accurate new method to measure specific heat at arbitrary temperature (quotient method)
Revue Phys. Appl. **13** 298

Moses D, Ben-Aroya O and Lupu N 1976 Simple calorimetric system for the temperature range 3–300 K with on-line computer
Rev. Sci. Instrum. **48** 1098

Pawels R E and Stansbury E E 1965 The specific heat of copper, nickel and copper–nickel alloys
J. Phys. Chem. Solids **26** 607

Pompe G and Hegenbarth E 1968 A calorimeter for the determination of specific heat between 4 and 150 K by a dynamic measuring method
Cryogenics **8** 309

Yagfarov M Sh 1968 New method of measuring heat capacity at low temperatures
Sov. Phys. – Dokl. **13** 265